Spatiotemporal Mapping of Cortical Activity Accompanying Voluntary Movements Using an Event-Related Beamforming Approach

Douglas Cheyne,* Leyla Bakhtazad, and William Gaetz

Neuromagnetic Imaging Laboratory, Hospital for Sick Children Research Institute, Toronto, Ontario, Canada

Abstract: We describe a novel spatial filtering approach to the localization of cortical activity accompanying voluntary movements. The synthetic aperture magnetometry (SAM) minimum-variance beamformer algorithm was used to compute spatial filters three-dimensionally over the entire brain from single trial neuromagnetic recordings of subjects performing self-paced index finger movements. Images of instantaneous source power ("event-related SAM") computed at selected latencies revealed activation of multiple cortical motor areas prior to and following left and right index finger movements in individual subjects, even in the presence of low-frequency noise (e.g., eye movements). A slow premovement motor field (MF) reaching maximal amplitude ~50 ms prior to movement onset was localized to the hand area of contralateral precentral gyrus, followed by activity in the contralateral postcentral gyrus at 40 ms, corresponding to the first movement-evoked field (MEFI). A novel finding was a second activation of the precentral gyrus at a latency of ~150 ms, corresponding to the second movement-evoked field (MEFII). Group averaging of spatially normalized images indicated additional premovement activity in the ipsilateral precentral gyrus and the left inferior parietal cortex for both left and right finger movements. Weaker activations were also observed in bilateral premotor areas and the supplementary motor area. These results show that event-related beamforming provides a robust method for studying complex patterns of time-locked cortical activity accompanying voluntary movements, and offers a new approach for the localization of multiple cortical sources derived from neuromagnetic recordings in single subject and group data. *Hum Brain Mapp 27:213–229, 2006.*

Key words: magnetoencephalography; beamformers; voluntary movements; motor cortex; proprioception; motor preparation

INTRODUCTION

Magnetoencephalographic (MEG) recordings of brain activity accompanying the performance of voluntary, self-paced movements show a complex spatiotemporal pattern of activity from multiple brain regions. Slowly changing neuromagnetic fields preceding voluntary movement (readiness or motor fields) are typically widely distributed over the scalp even for isolated movements of individual digits, and are presumed to arise from bilateral regions of the sensorimotor cortex [Cheyne and Weinberg, 1989; Kristeva et al., 1991]. Whole-head MEG recordings have confirmed bilateral activation near or in the precentral gyrus [Babiloni et al., 2001; Cheyne et al., 1995; Taniguchi et al., 1998], although there is some debate as to how consistently ipsilateral premovement fields can be observed, and whether they represent activity within the primary motor area [Huang et al., 2004; Nagamine et al., 1996; Volkmann et al., 1998]. Dipole modeling studies based on EEG recordings

Contract grant sponsor: Canadian Institutes of Health Research; Contract grant number: MOP 64279 (to D.C.).

*Correspondence to: Dr. Douglas Cheyne, Department of Diagnostic Imaging, The Hospital for Sick Children, 555 University Ave., Toronto, Ontario M5G 1X8, Canada.
E-mail: douglas.cheyne@utoronto.ca

Received for publication 24 February 2005; Accepted 25 May 2005
DOI: 10.1002/hbm.20178
Published online 21 July 2005 in Wiley InterScience (www.interscience.wiley.com).

[Bocker et al., 1994; Toma et al., 2002; Toro et al., 1993] have also provided evidence of a bilateral activation of motor areas during finger movements, although the precise anatomical locations of these sources is unclear given the difficulty of constructing accurate EEG forward solutions. More recent EEG and MEG modeling studies employing distributed current solutions and realistic head models [Babiloni et al., 2001; Ball et al., 1999] have shown activation of bilateral primary motor cortex during voluntary finger movements, although these methods require time-consuming cortical segmentation techniques. Slow premovement fields are followed by transient responses accompanying the onset of electromyographic activity in the involved muscles, termed movement-evoked fields [Cheyne and Weinberg, 1989; Kristeva et al., 1991]. The earliest and most consistent movement-evoked field (MEFI) occurs 30–40 ms following movement onset (about 100–120 ms following onset of EMG activity) and has been proposed to reflect sensory feedback to cortex from the periphery [Cheyne et al., 1997]. MEG dipole modeling studies have provided evidence that the MEFI arises from locations in the postcentral gyrus consistent with activation of area 3b in the posterior wall of the central sulcus, an area that receives afferent input from cutaneous and joint receptors [Kristeva-Feige et al., 1995; Oishi et al., 2004], although removal of cutaneous input does not abolish the MEFI response [Kristeva-Feige et al., 1996], indicating that proprioceptive input to area 3a might also contribute to its generation. Other MEG studies have failed to find evidence for a postcentral gyrus source of the MEFI [Ganslandt et al., 1999; Woldag et al., 2003]. Movement-evoked fields at latencies greater than 100 ms (e.g., MEFII and MEFIII) have rather complex topographies and their generators have not yet been identified.

Although MEG and EEG studies have modeled sources of time-locked movement-related brain activity primarily in the sensorimotor cortex, neuroimaging studies of voluntary movement tasks using functional magnetic resonance imaging (fMRI) or positron emission tomography (PET) typically show activation of multiple secondary motor areas, including lateral and medial premotor areas of the frontal lobes thought to be critical in the initiation of movements [Fink et al., 1997; Joliot et al., 1999]. More recently, MEG studies utilizing spatial filtering techniques have localized changes in ongoing oscillatory brain activity to nonprimary motor areas during motor tasks [Gross et al., 2005; Pollok et al., 2005]. EEG studies have successfully modeled activation of the supplementary motor area (SMA) during the premovement period [Babiloni et al., 2001; Ball et al., 1999]. MEG studies, on the other hand, typically detect only weak activity in the frontal midline [Erdler et al., 2000], presumably due to cancellation of tangential currents in the opposing hemispheres [Cheyne and Weinberg, 1989; Lang et al., 1991] and, to date, only a few MEG studies of time-locked motor responses have reported activation of anterior premotor areas [Huang et al., 2004; Pedersen et al., 1998].

Many of the inconsistencies in MEG and EEG source modeling studies of voluntary movement stem from the difficulty in localizing simultaneously active sources with overlapping temporal patterns of activity, and in close proximity to each other (e.g., sources in the hand representation area of the precentral and postcentral gyrus). In addition, these methods are extremely sensitive to slow magnetic field artifacts present in the data and require extensive editing of the data to remove artifacts (e.g., eye movements) even in cooperative, well-trained subjects. This makes localization of movement-related brain activity particularly problematic in patient populations and children, and excessively time-consuming for use in clinical settings. MEG studies of motor preparation offer superior temporal and spatial resolution to other methods; however, current source reconstruction approaches still suffer from difficulties in modeling complex configurations of sources. In order to model electrical brain activity with minimal interference due to simultaneously active sources, spatially filtering approaches have been proposed based on a technique known as beamforming [Van Veen et al., 1997] and various types of beamforming algorithms have been recently adapted to neuromagnetic measurements [Gross et al., 2001; Robinson and Vrba, 1999; Sekihara et al., 2001]. Beamforming is an array processing method that is able to take advantage of the high dimensionality of signal space afforded by multichannel MEG systems to achieve optimal suppression of other brain sources, provided these sources are not highly correlated (synchronous) with the target source during the time period of analysis. Since this approach does not require specifying the number of interference sources or their forward solutions, it has the advantage of potentially attenuating all sources of spatially correlated noise in the data (e.g., eye movements) without having to specify their location or the configuration of the underlying currents.

A number of recent studies have applied the synthetic aperture magnetometry (SAM) beamformer algorithm described by Robinson and Vrba [1999] to the localization of brain activity. These studies used the SAM beamformer to create differential images of source power changes over discrete time intervals and frequency bands, relative to baseline activity, to localize brain activity associated with self-paced movements [Cheyne and Gaetz, 2003; Taniguchi et al., 2000] or responses to sensory stimuli [Fawcett et al., 2004; Gaetz and Cheyne, 2003; Herdman et al., 2004; Hirata et al., 2002; Schulz et al., 2004]. However, this approach sacrifices temporal resolution by integrating power over relatively long (e.g., 200 ms) time windows. Hashimoto et al. [2001, 2003] used a different beamforming technique [Sekihara et al., 2001] to image brain activity at single time points in the somatosensory cortex and cerebellum from averaged MEG responses to median nerve stimulation. Similar approaches using the SAM beamformer algorithm have been recently proposed [Bardouille et al., 2004; Robinson, 2004]. Here we describe the application of the SAM beamformer algorithm to the imaging of instantaneous, time-locked source activity, which we term "event-related SAM" (ER-SAM), in order to describe spatiotemporal patterns of brain activity accompanying simple voluntary finger movements. Preliminary re-

sults of this study have been presented in abstract form [Bakhtazad et al., 2004].

SUBJECTS AND METHODS

Spatiotemporal Source Analysis Using Minimum-Variance Beamforming

A beamformer is a spatial filter designed to detect a signal corresponding to a specified location and attenuate signals from all other locations. For localization of brain activity, the signal of interest is defined by the forward solution for a current dipole source at each location (target voxel). Adaptive or minimum-variance beamformers achieve optimal attenuation of other sources in a least-squares sense based on spatial correlations present in the measured data, and the spatial resolution of the beamformer is dependent on the signal-to-noise ratio (SNR) of the target source. In addition, beamformer construction assumes that sources are uncorrelated and therefore detects only that portion of the target signal that is uncorrelated with signals from other sources. In the absence of anatomical constraints, the direction of current flow (dipole orientation) at each target voxel is unknown. One approach is to compute separate beamformer weights for orthogonal dipole orientations resulting in multidimensional arrays of weights [Van Veen et al., 1997]. For the current method, we used the synthetic aperture magnetometry (SAM) beamformer algorithm proposed by Robinson and Vrba [1999] that derives a single optimal dipole orientation vector **u** at each target voxel that produces the maximal ratio of power-to-noise output. This has the advantage of realizing higher SNR than multidimensional beamformers [Sekihara et al., 2004; Vrba and Robinson, 2001] while avoiding time-consuming calculations of anatomical constraints that require highly accurate coregistration procedures [Hillebrand and Barnes, 2003]. The beamformer for each location **r** consists of a unique set of sensor coefficients, or weights, denoted **w(r)**. These weights can be obtained by solving for the minimization of total source power $S^2(\mathbf{r})$ while retaining unit gain for the forward solution denoted **B(r,u)**:

$$\min_{\{w(r)\}} S^2(\mathbf{r}) = \mathbf{w}^T(\mathbf{r})\mathbf{C}\mathbf{w}(\mathbf{r}) \quad \text{subject to } \mathbf{B}(\mathbf{r},\mathbf{u})\mathbf{w}^T(\mathbf{r}) \equiv \mathbf{1} \quad (1)$$

where **C** is the covariance matrix based on the nonaveraged measured signals for all data segments of interest, and *T* denotes transpose. If the data covariance is well estimated (sufficient number of time samples), then the inverse of **C** can be obtained without regularization and the weight vector **w(r)** that provides maximum spatial resolution of the filter (minimum source interaction) is given by [Van Veen et al., 1997]:

$$\mathbf{w}(\mathbf{r}) = \frac{\mathbf{C}^{-1}\mathbf{B}(\mathbf{r},\mathbf{u})}{\mathbf{B}^T(r,u)\mathbf{C}^{-1}\mathbf{B}(r,u)} \quad (2)$$

It should be noted that the beamformer weights are unable to suppress *uncorrelated* noise, which will be amplified in a spatially nonuniform manner due to rapidly decreasing signal strength with increasing distance from the sensors, distorting beamformer images [Van Veen et al., 1997]. This distortion can be removed by normalizing the beamformer output by an estimated amount of uncorrelated noise projected through the weights. Noise normalized estimates of source power derived from beamformer filters and have been termed the "pseudo-Z" [Robinson and Vrba, 1999] or the "neural-activity index" [Van Veen et al., 1997]. This correction can also be applied to the beamformer weights prior to computing source power:

$$\|\mathbf{w}(\mathbf{r})\| = \frac{\mathbf{w}(\mathbf{r})}{\sqrt{\sum_{i=0}^{M}(wi(\mathbf{r})n_w)^2}} \quad (3)$$

where $\|\mathbf{w}(\mathbf{r})\|$ represents the noise normalized weight vector, and the uncorrelated noise in the bandwidth of the measurement, n_w is constant across *M* sensors. These normalized weights can be applied to the measured signal vector, $\mathbf{m}(t) = [m_1(t), m_2(t) \ldots m_M(t)]$ that represents the recorded MEG signals from *M* sensors as a function of time *t*, to produce a time series (*virtual sensor*) of the estimated source power $\hat{\mathbf{S}}(\mathbf{r},t)$ at the target location **r** without spatial smearing,

$$\hat{\mathbf{S}}(\mathbf{r},t) = \|\mathbf{w}^T(\mathbf{r})\|m(t) \quad (4)$$

Event-Related SAM

Figure 1A illustrates the calculation of averaged virtual sensor time series using the SAM beamformer algorithm. Normalized beamformer weights for each voxel location in the brain are derived from the covariance matrix of the unaveraged single trial data for all trials and all time samples using Eqs. 2 and 3. The forward solution was based on a homogeneous conducting sphere [Sarvas, 1987] and utilized the multiple sphere method based on the extracted MRI head surface for each subject to reduce inaccuracies due to nonspherical head shape [Huang et al., 1999]. The estimate of uncorrelated noise level $\mathbf{n}_w$ was derived directly from the data, based on the smallest singular value of a singular value decomposition (SVD) of the time data across all chosen time windows [Robinson and Vrba, 1999]. This yielded a consistent noise constant across subjects of approximately 3 $fT_{rms}/\sqrt{Hz}$. It should be noted, however, that this value acts as a constant scaling factor across all voxels and can be derived by other means, with no significant change in the spatial distribution of source activity. Optimal dipole orientation **u** is then determined iteratively by adjusting the dipole orientation (reducible to a single tangential angle for MEG) and recalculating the beamformer weights to maximize virtual sensor total power over all epochs [Robinson and Vrba, 1999]. The resulting normalized beamformer weights are used to produce a virtual sensor time series for

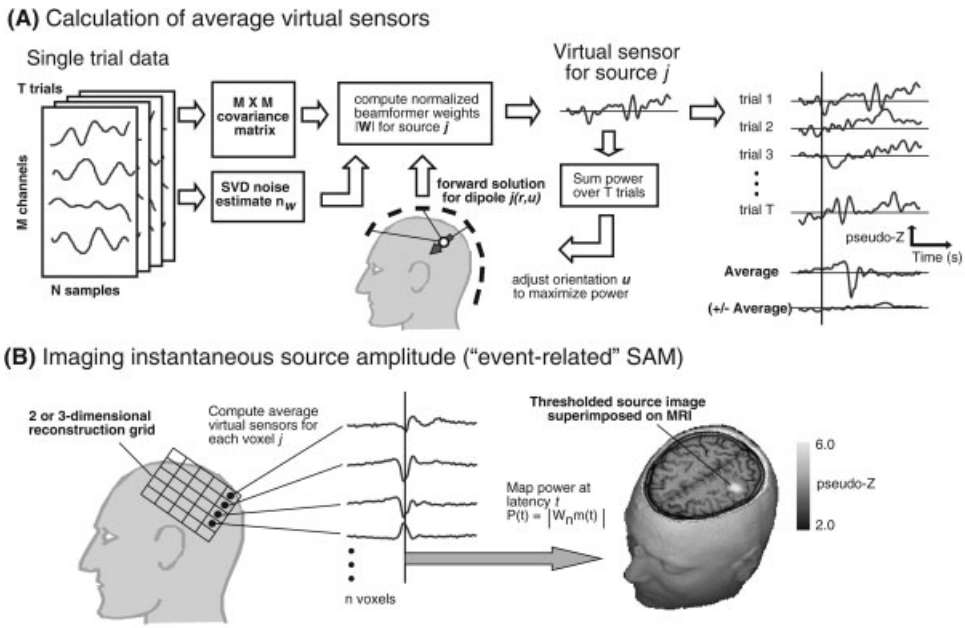

Figure 1.

A: Calculation of averaged virtual sensors using the SAM minimum-variance beamformer algorithm for a single dipole location in the head as indicated by the solid arrow. The beamformer weights are derived from the covariance matrix based on the unaveraged single trial data and normalized by the estimated uncorrelated noise n_w (left). Dipole orientation **u** is then iteratively adjusted to maximize total source power integrated over all trials (center). The virtual sensors for the optimal source orientation are then averaged across trials with respect to a stimulus event shown by the vertical line (right). The plus-minus average (± Average) is also computed by multiplying odd numbered trials by −1.0. **B:** Virtual sensors are computed for each node of a 2D or 3D lattice of n voxels covering a region of interest (left). Virtual sensor amplitude at selected latencies is rectified and mapped onto the subject's MRI scan. The amplitude map of the 20-ms response to electrical median nerve stimulation of the right wrist is shown superimposed on the axial slice through the primary somatosensory cortex in one subject.

this location using Eq. 4. As shown in Figure 1A (right), these time series are then averaged over trials, time-locked to a stimulus event (note that since Eq. 4 represents a linear transformation of the data, the weights can also be applied directly to the averaged data). Similarly, the plus-minus average can be calculated to provide an estimate of the nonstimulus-locked source activity projected by the spatial filter.

Figure 1B shows the procedure for calculation of a volumetric event-related SAM (ER-SAM) image for a selected latency from the averaged virtual sensor waveforms. The spatial distribution of source amplitude at time sample *t* was sampled over a 3D lattice of virtual sensors over a chosen region of interest and resolution and the extracted source amplitude saved as a single volumetric image in units of noise normalized source power (pseudo-Z). Since dipole orientation in the SAM algorithm is derived from source power, absolute polarity of the dipole is unknown and may be randomly assigned across neighboring voxels. As a result, beamformer amplitude must be rectified prior to computing volumetric ER-SAM images. However, the true source polarity for individual voxels identified in the ER-SAM images can often be recovered (e.g., by inspection of topographic maps). The image shown in Figure 1B (lower right) shows the event-related SAM image for the N20m response to right median nerve stimulation in a single subject overlaid on the subject's MR image.

Subjects

Nine healthy right-handed subjects (seven male, two female, ages 21–46) participated in this experiment. All subjects were recruited from the Toronto area and provided informed consent using protocols approved by the Hospital for Sick Children Research Ethics Board. The data from one participant was excluded due to large variability in the timing of their movements.

MEG Recordings

Neuromagnetic activity was recorded using a whole-head 151 channel MEG system (Omega-151; VSM Medtech, Vancouver, Canada) in a magnetically shielded room. Data were collected at a sample rate of 625 samples/s and a bandpass of 0–200 Hz. Subjects sat upright in an adjustable chair with eyes open and looking at a fixation point. Prior to MEG data acquisition, each subject was fitted with three fiducial localization coils placed at the nasion and pre-auricular points in order to localize the position of the subject's head relative to

the MEG sensors. Coil placements were carefully measured and photographed for off-line coregistration of the recorded MEG data to structural MR images obtained for each subject.

Subjects pressed a button on a nonmagnetic fiber optic response pad (LUMItouch Response System, Lightwave Medical Industries, Burnaby, Canada) placed on armrests on either side of the subject with their right or left index finger at their own pace, without counting. A barrier obstructed the subject's view of their lower arms and hands, and foam earplugs were used to minimize acoustic artifacts from the response pad. The timing of movements was monitored throughout the recording and subjects were instructed to increase or decrease their movement rate such that their intermovement interval was ~8–10 s. The nonmoving hand rested on the opposite armrest and care was taken to avoid mechanical vibrations from the moving hand that might elicit time-locked ipsilateral sensory responses [Cheyne et al., 1997]. Eighty movements were recorded for both left and right index fingers in separate recordings, counterbalanced across subjects. Depressing the response pad button triggered acquisition of 6-s trials with a 4-s pretrigger period. In one subject the recordings were conducted with bipolar surface electromyogram recorded from right and left forearm flexors, and EOG recorded diagonally over the left eye.

Somatosensory Evoked Fields

After completing the movement tasks, responses to left and right median nerve stimulation were recorded for each subject using 0.2 ms duration constant current square wave pulses delivered transcutaneously at the wrist above motor threshold, at a rate of 3.1 stimuli per second; 600 epochs of 200 ms duration (50 ms prestimulus baseline) were collected at a sample rate of 2,500 samples/s (DC to 800 Hz bandpass). SEF responses were bandpass filtered (15–300 Hz) and averaged. Structural (T_1-weighted, 3D-SPGR) MRI scans were obtained for each subject using a 1.5T Signa Advantage System (GE Medical Systems, Milwaukee, WI). A spherical model was manually fit to the inner skull surface based on each subject's MRI. A single dipole model was fit to the "N20m" peak, observed over the contralateral somatosensory cortex, using a least-squares minimization algorithm (CTF DipoleFit). Coregistration of the MEG head based coordinate system with the MR images was achieved by identifying the locations of the head localization coils on orthogonal slices of each subject's MRI. Locations for the N20m dipole fits were then superimposed on the MR image.

ER-SAM Imaging and Group Analysis

In the current study ER-SAM images with a spatial sampling resolution of 3 mm were computed for the whole head, or slightly higher resolution (2 mm) resolution images for smaller regions of interest around the hand areas of sensorimotor cortex. The entire epoch duration of single-trial data was used to estimate the data covariance after bandpass filtering from DC to 30 Hz. ER-SAM images were created at 5-ms increments preceding and following movement onset and individual images were scanned to find peak activations. For peak locations of activity in the ER-SAM images, averaged time series (*virtual sensor*) waveforms were reconstructed for the entire epoch in order to examine source activity as a function of time.

Methods for group averaging of SAM functional images based on spatial normalization techniques have been previously described [Chau et al., 2004; Singh et al., 2003]. Spatial normalization to the MNI (*T*1) template brain was carried out using SPM99 (Welcome Institute of Cognitive Neurology, London, UK). Both linear and nonlinear warping parameters were obtained from each individual's T_1-weighted MR scans, then applied to volumetric SAM images for selected latencies, which were resampled to produce 3-mm resolution images of source power in standardized stereotactic space, then averaged across subjects. Group images were superimposed on the MNI (CH) template brain [Collins et al., 1994] using the mri3dX program (http://www.aston.ac.uk/lhs/research/nri/groups/nrg/mri3dx/index.jsp) to view 2D or 3D (rendered) images of the ER-SAM functional images in template space. Talairach coordinates of peaks activations were determined from the normalized images using the MNI to Talairach daemon [Lancaster et al., 2000].

In order to view the entire time course of activity for a voxel location of interest in the group averaged data, deformation fields were created for each subject that provided the inverse transformation from Talairach coordinates to locations in the individual subject's head based (MEG) coordinate system. These coordinates were then used to generate average virtual sensor waveforms based on each subject's data, and these virtual sensors for peak locations averaged across subjects to produce grand averages of virtual sensors.

RESULTS

All subjects showed premovement slow shifts (readiness and motor fields) followed by movement-evoked fields in the averaged MEG waveforms at latencies consistent with those described in the literature. A slow readiness field (RF) was observed in all subjects, beginning as early as 2 s prior to movement onset (time = 0 s) in some subjects. This was followed by an increase in slope, termed the motor field (MF), beginning ~500 ms prior to movement and reached maximal amplitude 50–60 ms prior to movement. Figure 2A shows a typical response for a right index finger movement in one subject for a selected MEG sensor over the contralateral motor cortex. Note that the topography of the MF was usually bilaterally distributed over the head (Fig. 2A, right). This was followed by a highly dipolar field pattern over the contralateral hemisphere, characteristic of the first movement-evoked field (MEFI) component at a latency of 40 ms following movement onset. The MEFI was followed by a second movement-evoked field (MEFII) at a latency ranging from 130–160 ms that typically showed a more complex topographic pattern over the scalp.

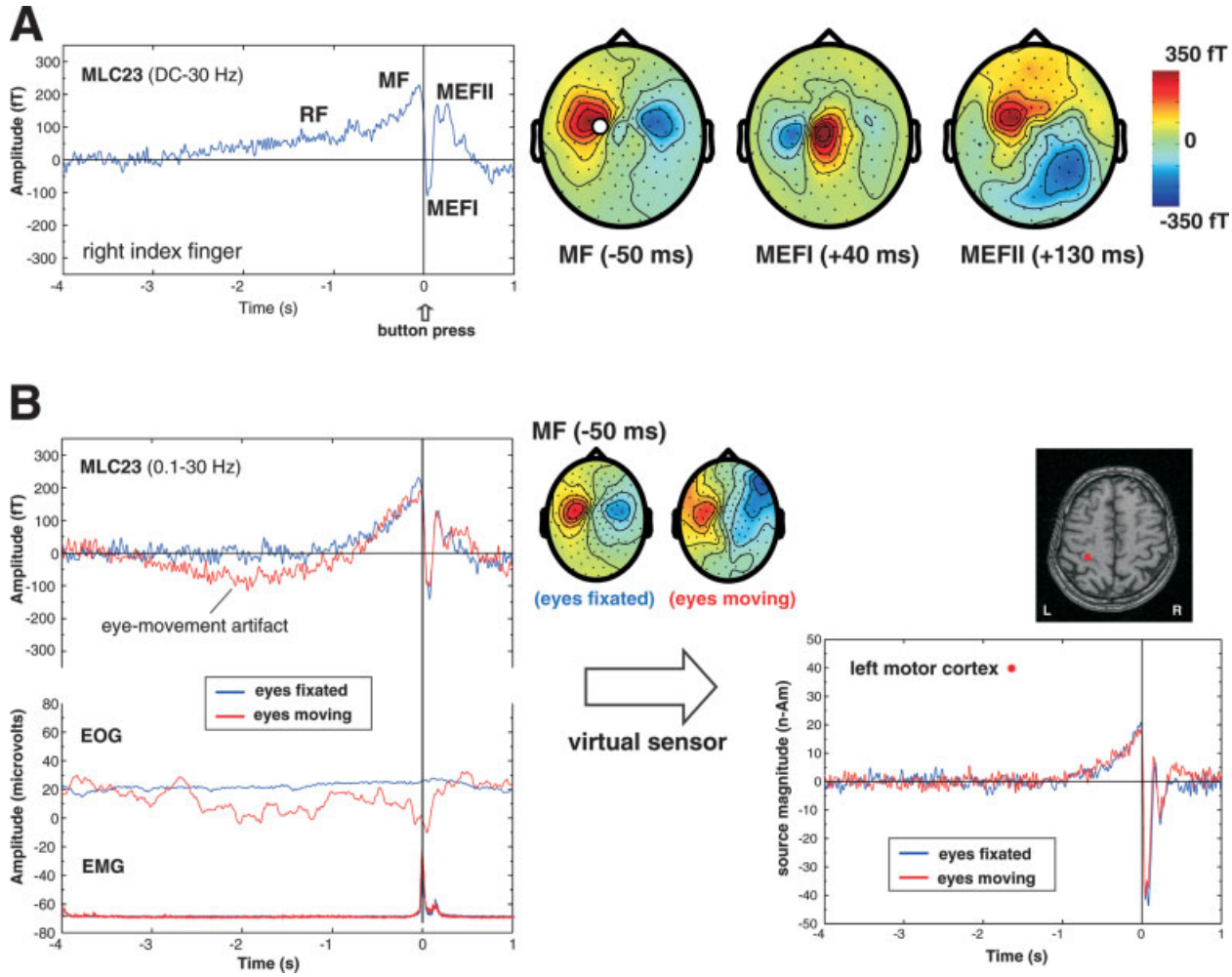

Figure 2.

A: Time average of the movement-related magnetic fields (BW = DC to 30 Hz) for right index finger flexions (button-press) in one subject for a channel overlying the contralateral sensorimotor area (MLC23). RF = readiness field, MF = motor field, MEFI and MEFII = first and second movement-evoked fields. Averages were time locked to the button press (t = 0 s) for 80 movements. The topographic field patterns (nose upwards) of the MF, MEFI, and MEFII are shown on the right with the location of channel MLC23 shown by the white circle (red = outgoing fields, blue = ingoing fields, fT = femtoTesla). **B:** Effects of eye movement (blue traces) compared to fixation (red traces) on the averaged MEG response for the same subject and channel as shown above. Note the presence of a slow drift in the baseline and distorted topographic pattern of the MF that is not removed by additional high-pass filtering (0.1 Hz) due to increased eye movement artifact as shown in the electrooculogram (EOG) recorded diagonally over the left eye. In contrast, the SAM virtual sensors for the MF source on the right show no effect of eye movement artifacts on the virtual sensor baseline or amplitude. Surface electromyogram recorded from the forearm flexors (EMG) shows the onset of muscle activity preceding the button press by ~80 ms.

Low-Frequency Noise Reduction

In some subjects the averaged MEG waveforms and topographic maps were clearly distorted by low-frequency contamination due to eye movements or environmental noise (e.g., automobile traffic from a nearby road) even when utilizing combined adaptive balancing and third-order synthetic gradient noise reduction [Vrba and Robinson, 2001]. Since these artifacts have similar frequency characteristics to the brain responses of interest, they would normally require excluding large numbers of trials, or even entire datasets. In order to determine the ability of the beamformer algorithm to separate brain activity from these sources of noise, an additional experiment was conducted in a well-trained subject while they either carefully avoided eye movements ("eyes fixated") or purposefully made random eye movements ("eyes moving") while performing the button-pressing task. EOG recordings confirmed the stability of eye position during the recordings. Figure 2B demonstrates the

difference in the averaged waveform for the same MEG sensor (MLC23), showing a large DC drift in the average for eyes moving condition (red traces) in comparison to the fixation condition (blue traces) and a corresponding distortion of the topography of the MF as seen in the topographic maps. This is presumably due to slow eye movement as seen in the averaged EOG signal shown in Figure 2B. Virtual sensors calculated for a location in the contralateral hand area of the precentral gyrus for both conditions are compared in Fig. 2B (right panel). Note that the virtual sensors show no DC drift during the baseline or premovement periods and are identical across the two conditions. As a result, trials containing eye movement or slow noise artifacts were not excluded from further analysis.

Surface EMG from the forearm flexors was also recorded in this subject. Figure 2B shows the averaged rectified EMG signal time-locked to the optical button trigger with similar onset of the EMG burst from the active muscles across conditions. EMG onset was ~80 ms prior to physical displacement of the finger as measured by the button press (t = 0 s) ms. MEFI peak latency was ~40 ms in this subject, consistent with previously reported MEFI latencies ranging from 100–120 ms following EMG onset.

Spatiotemporal Analysis Using ER-SAM

Activation of the contralateral sensorimotor cortex

All subjects showed a very similar spatiotemporal sequence of source activity in the event-related SAM images located in the region of the anatomically defined hand area or "motor knob" [Yousry et al., 1997] in the hemisphere contralateral to the side of movement. This began with a slow increase in activity in the precentral gyrus that reached maximal amplitude ("MF peak") just prior to movement onset (mean latency = –55 ± 18.7 ms for left and right hand combined) with a significantly earlier peak latency ($P < 0.05$) for right index finger movements (–60.6 ± 10.6 ms) vs. left index finger movements (–44.8 ± 14.6 ms). This was followed by a very strong and brief period of activity immediately following movement onset located in the anterior portion of the postcentral gyrus. This activity reached maximal amplitude around 40 ms after movement onset (left index finger, 44.4 ± 11.2 ms; right index finger, 42.6 ± 14.8 ms) and corresponds in latency to the highly dipolar MEFI observed in the time data. This "MEFI peak" was followed by another strong burst of activity ("MEFII peak") that shifted in location back to the precentral gyrus, close in location to the MF peak location reaching maximum amplitude about 150 ms following movement onset (left index finger, 146.6 ± 8.6 ms; right index finger, 145.6 ± 7.5 ms). The MEFI and MEFII peaks were not statistically different in latency between left and right finger movements and were remarkably similar in latency for the MEFII. In some subjects the MEFI activity in the postcentral gyrus continued during the MEFII, or more rarely was weakly active prior to movement onset. Figure 3A shows an example of a typical spatiotemporal sequence in one subject. The averaged virtual sensors for the peak locations of the MF, MEFI, and MEFII (identical to the MF in this case) for right index finger movements are shown below the ER-SAM images. Note that the virtual sensor for the MEFI (middle trace) shows an increase in activity during the period of the MEFI only, with no slow premovement shift, whereas the MF and MEFII source waveforms show slow premovement shifts and increases corresponding to the latencies of the MF and MEFII, but no activity during the MEFI.

In order to further quantify the relative anatomical location of the MF, MEFI, and MEFII, peak ER-SAM locations were transformed to a common coordinate system based on the location of the fitted N20m dipole location for median nerve stimulation of the corresponding hand in each subject. This allowed us to plot the mean location of each peak across subjects, relative to their N20m location in the same hemisphere. In all subjects the N20m dipole locations were located in the postcentral gyrus, slightly lateral to the hand motor knob. Figure 4 shows a 3D representation of the mean location for MF, MEFI, and MEFII peaks in this normalized coordinate system. The mean MF peak was found to be anterior and medial, and the MEFI peak posterior and medial, to the N20m dipole location for both left and right finger movements. The MEFII peak location was found to be also slightly anterior to the N20m dipole, but posterior to the MF peak. Mean separation between the MF and MEFI was 0.91 cm and 1.01 cm, for left and right index finger movements, respectively, with the largest difference observed in the anterior–posterior direction (Table I) which was statistically significant across subjects ($P < 0.001$, corrected, t-test for paired differences). The MF was also slightly anterior and superior to the MEFII peak for both left and right index finger movements; however, this difference was not statistically significant at the $P < 0.05$ level.

Ipsilateral motor cortex activity

In almost all subjects significant activity was also measured in the hand area of the ipsilateral precentral gyrus for both right and left finger movements. Figure 2B shows 3D ER-SAM images of the MF peak activity in Subject 3 with a cutaway in the axial plane at the level of both peaks, revealing bilateral activation in the hand region of the precentral gyrus for both right and left index finger movements. The virtual sensors for ipsilateral ER-SAM peaks (middle traces) show that the ipsilateral activity consisted of a slow premovement shift that continued during movement onset. In contrast, the large MEFI response following movement onset was only present in the virtual sensors for the precentral sources contralateral to the side of movement.

Group SAM analysis of movement-related activity

Activation of the contralateral sensorimotor area was sufficiently robust in the ER-SAM images to be observable within individual subjects. Peak amplitudes of these sources were 3–4 times larger than background activity, as estimated from the maximal pseudo-Z values observed in ER-SAM images derived from the plus-minus data for ran-

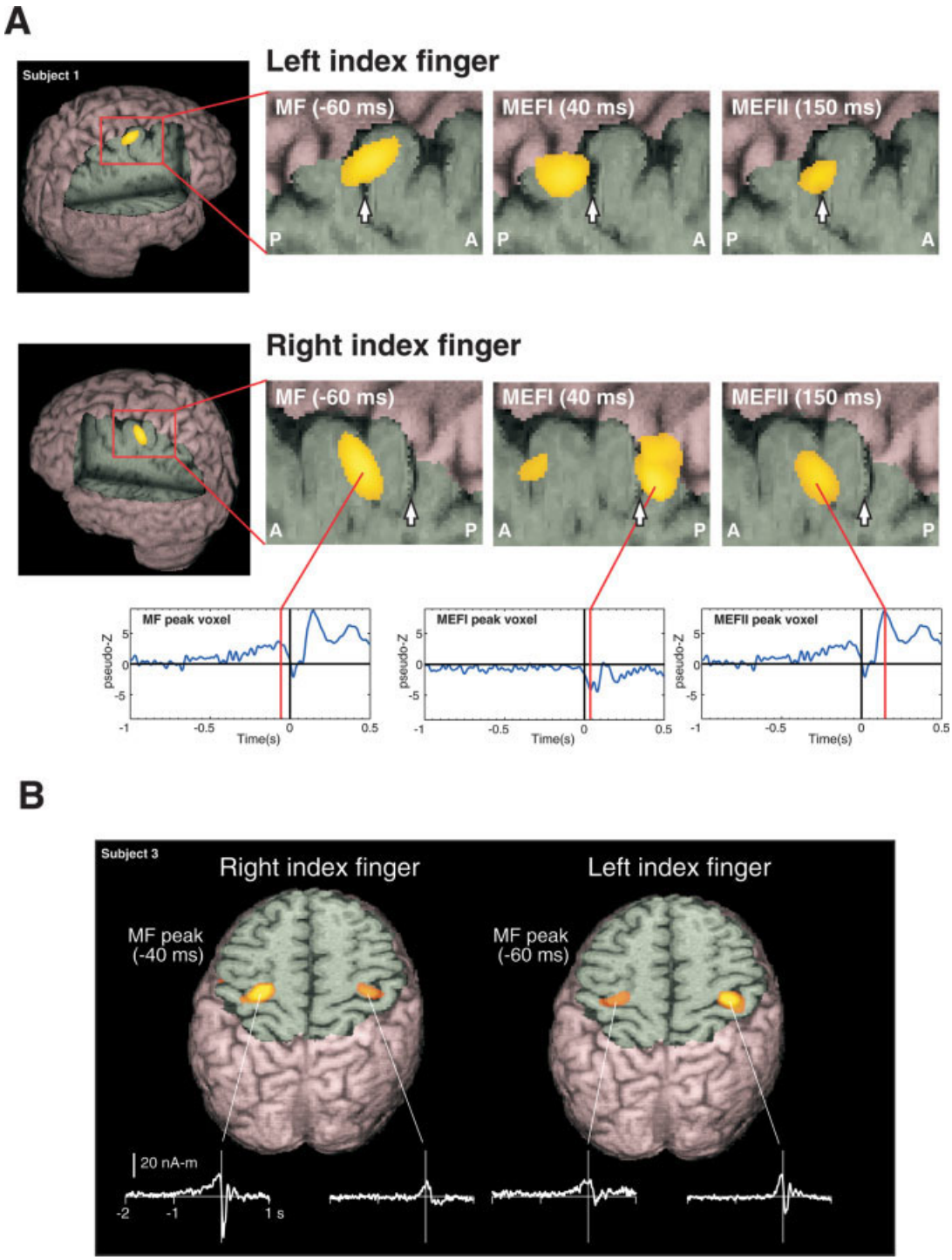

Figure 3.

A: Event-related SAM (ER-SAM) images of contralateral sensorimotor cortex activity created at 2-mm resolution for left and right index finger movements, superimposed on rendered MR images of a single subject. The location of the central sulcus is shown by a white arrow in the magnified views of contralateral sensorimotor areas, showing a shift in peak location of the MF, MEFI, and MEFII from precentral to postcentral locations. The averaged virtual sensor for the peak location for MF/MEFII and MEFI are shown below. **B:** ER-SAM images for left and right index finger movements in a single subject, superimposed on an axial MRI slice through the contralateral and ipsilateral hand region of the precentral gyrus. Shown below are the *non-noise normalized* average virtual sensor waveforms (in units of nanoAmpere-meters) for the peak locations in the primary motor cortex. Images were created using the mri3dX program.

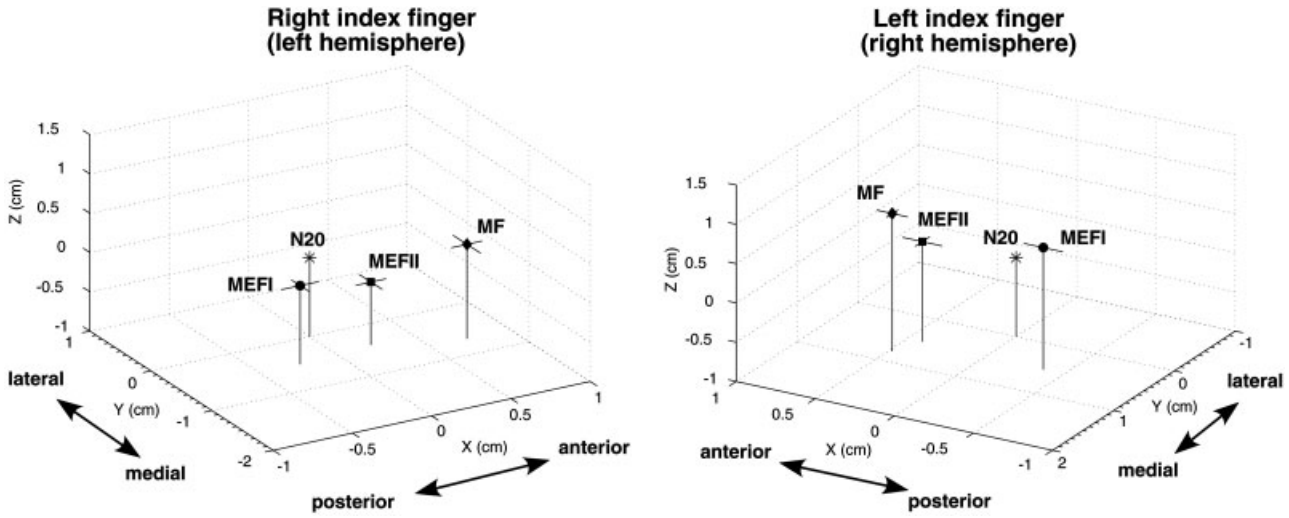

Figure 4.

Mean locations of motor field (MF), movement-evoked field I (MEFI), and movement-evoked field II (MEFII) peak locations from the ER-SAM images for right and left index finger movements for all eight subjects, plotted relative to an origin (0, 0, 0) defined by the location of the dipole fit to median nerve stimulation (N20m) of the same hand. The axes correspond to the MEG coordinate system (x = posterior to anterior, y = right to left, z = inferior to superior). Horizontal bars indicate 1 standard error of the mean in the x and y directions. Mean distances between peak locations are given in Table I.

domly selected time samples. However, weaker peaks of activity could also be observed in other brain areas that were more variable in location and amplitude and occasionally difficult to discern above noise in individual subjects. Group averaging was performed on 3-mm resolution ER-SAM images for the entire brain (n = 8 subjects) at fixed latencies for the MF (–50 ms) and MEFI (40 ms). Figure 5 shows the group averaged ER-SAM images for the MF peak for right and left index finger movements displayed as maximum intensity projection images. A nonparametric permutation test [Nichols and Holmes, 2002; Singh et al., 2003] of the whole-head ER-SAM images produced a statistical threshold with usually only one or two significant clusters of activation in the contralateral sensorimotor area. This was presumably due to bias of the permutation distribution by the relatively large pseudo-Z values for the MF or MEFI peaks that had amplitudes 2–3 times larger than other peaks visible in the images, with correspondingly large spread functions around the peak, as can be seen in Figure 5. In order to detect weaker areas of activation, two additional thresholding techniques were employed. First, event-related SAM images were computed at the peak latencies on the basis of the plus-minus averaged data and averaged across subjects. These images showed only diffuse deep activity, with a maximum pseudo-Z value of ~0.6 for both left and right finger conditions. Second, nonparametric permutation tests were applied to the group data for randomly selected latencies during the baseline period (–4 to –3 s), similar to the method described by Chau et al. [2004] resulting in maximum pseudo-Z values ranging from 0.4–0.5. Application of thresholds in these ranges still showed relatively diffuse activity in the MF and MEFI images due to the large activation in the contralateral hemisphere and spurious peaks in deeper locations. Thus, for the subsequent analysis we chose a more conservative pseudo-Z threshold of 1.0. This resulted in 5–6 clear peaks of activity in similar cortical locations for left and right index finger movements. This included the bilateral hand areas of the precentral gyrus (PreC(L) and PreC(R)), the bilateral dorsal premotor areas (PMA(L) and PMA(R)), the ipsilateral parietal lobe in the left hemisphere (IPL(L)) slightly lateral and inferior to the hand area, and weaker, less consistent peak in the left dorsal mesial cortex, near the region of the supplementary motor area (SMA). Group ER-SAM images computed for the MEFI latency showed peaks of activation at similar locations reflecting continued activity at these

TABLE I. Distances between peak locations of MF, MEFI, and MEFII

		Mean distances between peaks (cm)			
Condition	Peaks compared	Δx	Δy	Δz	Distance
Left index	MF-MEFI	0.85*	0.28	0.20	0.92
	MF-MEFII	0.08	0.30	0.48	0.57
Right index	MF-MEFI	0.98*	−0.20	0.20	1.02
	MF-MEFII	0.50	−0.28	0.40	0.69

MF = motor field, MEFI = movement-evoked field I, MEFII = movement-evoked field II. Spatial separations in x, y, and z directions are in the MEG coordinate system and Euclidean distance between peaks (Distance) = $(\Delta x^2 + \Delta y^2 + \Delta z^2)^{1/2}$. Significant differences indicated by * ($P < 0.001$ corrected, df = 7, *t*-test for paired differences).

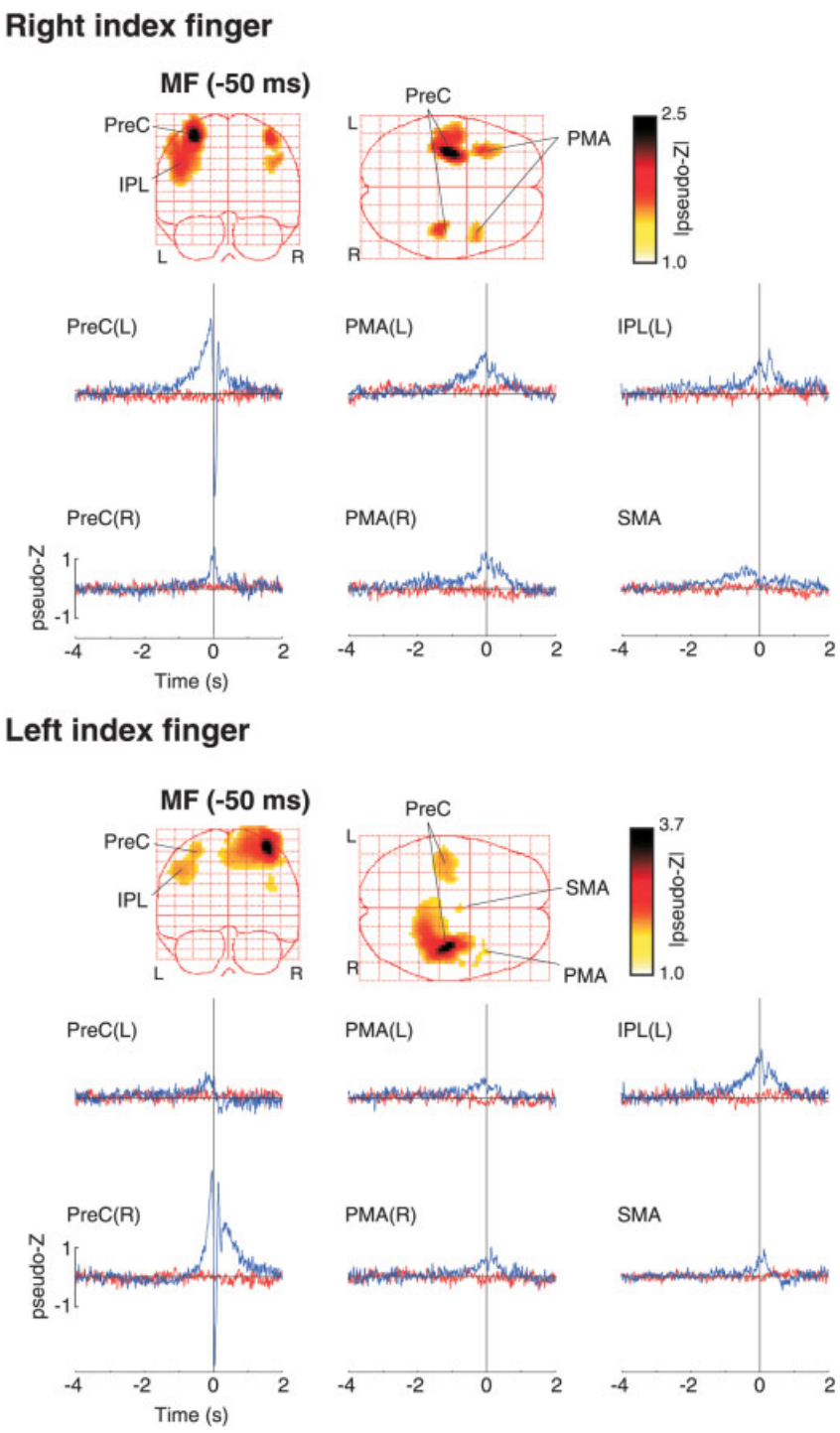

Figure 5.
Group ER-SAM images for right (top panel) and left (bottom panel) index finger movements (n = 8). The maximum intensity projections (left) of the motor field (MF) component (latency = –50 ms) averaged across subjects are shown with a pseudo-Z threshold value of 1.0. Six main peaks of activation were detected in the volumetric images in the right and left precentral gyrus, PreC(R) and PreC(L), the right and left lateral premotor areas, PMA(R) and PMA(L), the left inferior parietal cortex IPL(L) and the left supplementary motor area (SMA). The Talairach coordinates of these peak locations are given in Table II. The group averaged virtual sensors corresponding to the peak locations are shown in the plots below (blue traces). The red traces show the virtual sensors based on the plus-minus averages for the same locations.

locations throughout the movement, with the exception of the contralateral hand area that showed a shift in location toward the postcentral gyrus for both left and right finger movements, similar to that observed in the individual subject data. Talairach coordinates for the peak locations shown in Figure 5 are given in Table II.

Group averaged virtual sensors were computed for the peak locations identified in the group ER-SAM images, as

TABLE II. Talairach locations of peak activations in group averaged ER-SAM images

Brain area	Right index finger *x, y, z*	pseudo-Z	Left index finger *x, y, z*	pseudo-Z
MF (−50 ms)				
Left precentral gyrus	−33, −15, 59	2.51	−30, −17, 60	1.27
Right precentral gyrus	39, −21, 56	1.57	36, −17, 60	3.72
Left inferior parietal cortex	−45, −19, 37	1.66	−45, −21, 43	1.32
Supplementary motor area			0, 12, 66	1.09
Left premotor area	−33, 17, 49	1.46		
Right premotor area	45, 10, 35	1.22	39, 16, 24	1.05
MEFI (40 ms)**				
Left postcentral gyrus	−38, −22, 56	6.21		
Right postcentral gyrus			40, −23, 59	4.41

Mean locations and amplitudes of the six largest peak activations in the group averaged event-related SAM images preceding (MF) and following (MEFI) onset of left and right index finger movements. Talairach coordinates are presented (mm).

** For MEFI only the location of the largest peak in the contralateral hemisphere is listed, showing a posterior shift in peak location of the precentral gyrus sources. Peaks with pseudo-Z values < 1.0 were excluded.

described in Subjects and Methods. These waveforms are shown in Figure 5 (blue traces) overlaid on the virtual sensors for the plus-minus averaged data (red traces), showing the time course of activity in each of the identified peaks. It was noted that the time course of activity for precentral sites showed similar, but opposite patterns of activity for left and right finger movements, with a slightly later onset of the MF slow shift for left index finger movements. All locations show premovement activity, including the left hemisphere IPL that showed an early slow shift, similar to the premotor areas that continued during movement onset. The IPL peak was slightly obscured in the group image for right index finger movements (Fig. 5, top panel), but could be clearly discerned as a separate peak during weaker activation of the left precentral gyrus for the left finger movement condition (Fig. 5, lower panel). In addition, the time course for the left IPL source differed substantially from that of the nearby left precentral gyrus source, yet was similar for both left and right index finger movements.

DISCUSSION

The results of the current study indicate that the event-related beamforming method (ER-SAM) described here provides a more detailed description of the spatiotemporal pattern of activity within the contralateral sensorimotor cortex accompanying voluntary movements than has previously been shown. We observed robust activation of the precentral gyrus contralateral to the side of movement, even with a relatively small number of trials (80 movements). Virtual sensor analysis shows that this activity preceded movements by 0.5–1 s, reaching maximal amplitude at ~50 ms prior to movement onset as measured by a button press, corresponding roughly to the onset of muscle contraction [Kristeva et al., 1991]. This activity was followed by a brief and strong burst of activity in the postcentral gyrus that appears to reflect the main generator of the MEFI, consistent with previous dipole modeling studies [Kristeva-Feige et al., 1995; Oishi et al., 2004]. In a small number of subjects the precentral activity (MF source) remained active during the MEFI. A new finding in the current study, however, was a clear activation of the precentral gyrus, slightly posterior and deeper to the MF source location, at a latency of ~150 ms, corresponding in latency to the MEFII component identified in the surface MEG recordings. To our knowledge this is the first demonstration of a generator of the MEFII, and suggests that it arises, in part, from a second activation of the primary motor cortex following movement onset.

The mean location for the MF peak across subjects was found to be anterior and medial to the N20m dipole location for median nerve stimulation located in the postcentral gyrus [Kakigi et al., 2000]. This would support previous suggestions that the MF is generated in the primary motor cortex (area 4) in the anterior bank of the central sulcus and reflects activation of corticospinal neurons involved in descending output to the muscles [Ball et al., 1999; Cheyne and Weinberg, 1989; Kristeva et al., 1991]. However, fMRI and EEG modeling studies have shown that more anterior portions of the precentral gyrus, including area 6, are also active prior to movement onset [Hanakawa et al., 2004; Toma et al., 2002]. For example, Toma et al. [2002] presented a model in which there is a shift from area 6 activation in the crown of the precentral gyrus to area 4 in the sulcul wall prior to movement onset, reflecting sequential activation of neuronal populations involved in motor preparation to motor execution. These authors also speculated that, in comparison to EEG measures, MEG might reflect primarily activity in the sulcus due to insensitivity to radially oriented sources in the gyral surface, accounting for later onset of premovement magnetic field activity. Interestingly, we found that the MEFII source was slightly posterior and deeper to the MF

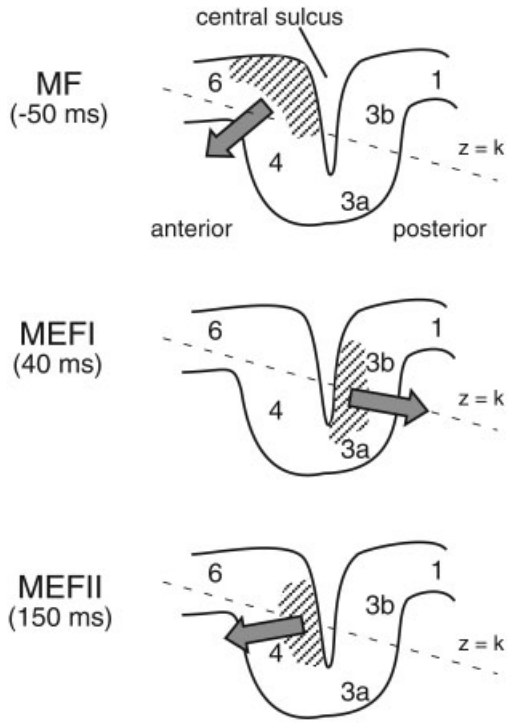

Figure 6.

Proposed generators of the motor field (MF) and first and second movement-evoked fields (MEFI and MEFII) relative to Brodmann areas of the contralateral sensorimotor cortex. Hatched areas indicate the regions of cortex activated during each of the three peak latencies and solid arrows the approximate vector sum direction of intracellular currents. The orientation of the x–y plane of the MEG coordinate system (z = constant) is tilted in the anterior–posterior direction as shown by the dotted line. See text for further details.

source, but also anterior to the N20m dipole, suggesting both MF and MEFII sources were located within different portions of the precentral gyrus. In contrast, the MEFI source lies posterior and medial to the N20m, ~1 cm posterior to the MF and MEFII sources, consistent with a location in the hand representation area of the primary somatosensory cortex in the postcentral gyrus.

Figure 6 shows a proposed model of the putative generators of the MF, MEFI, and MEFII within the contralateral sensorimotor area that may account for our current findings. These three sources were found to lie in a similar horizontal plane within the MEG coordinate system that is slightly tilted with respect to the cortical surface, with the MF source slightly anterior and superior to the MEFI and MEFII. In this model the slow premovement MF shift reflects activation of both superior and inferior portions of the precentral gyrus, with net current direction in the tangential direction that will vary across individuals. This would explain both a somewhat anterior location of the MF source, depending on the relative contribution of the crown of the precentral gyrus and the observation of very weak premovement fields in some subjects, as suggested in previous studies [Nagamine et al., 1996]. The activation of the more anterior portion of the precentral gyrus would also imply activation of neurons in area 6 related to motor preparation, rather than the somatotopically organized corticospinal output from area 4, as suggested in a recent fMRI study for ipsilateral hand movements [Hanakawa et al., 2004]. This interpretation would also be consistent with our recent observation of oscillatory changes in the hand area of the precentral gyrus during movements of the toe [Cheyne and Gaetz, 2003], suggesting that there are neuronal populations in the hand region in the precentral gyrus that may be related to general aspects of motor preparation that are co-activated with more somatopically specific output neurons of area 4.

As shown in Figure 6 (middle), the MEFI source is proposed to reflect activation of the posterior wall of the central sulcus, reflecting activation of tactile and proprioceptive afferent input to areas 3b and 3a, respectively. Since the movement task in the current study involved physical contact of the finger with a button, tactile input to more superior aspects of the sulcul wall might account for the relatively superior location of the MEFI source in some subjects, although contributions proprioceptive input cannot be ruled out. This result does not support suggestions of a precentral source of the MEFI by Woldag et al. [2003], who showed a preponderance of precentral locations of the MEFI across subjects using an L1 minimum-norm localization technique. However, the source locations in the latter study showed a rather large variability across subjects, with locations both anterior and posterior to the central sulcus. In contrast, we found a relatively small (<2 cm) but statistically significant shift in the mean location of the MEFI peak in relation to the premovement MF peak in close vicinity to the central sulcus in our group data, and MEFI activity in the ER-SAM images could be clearly located in the postcentral gyrus in individual subjects, consistent with the results of a recent dipole modeling study [Oishi et al., 2004].

The MEFII component is proposed to reflect a second activation of the precentral gyrus in closer proximity to the anterior wall of the central sulcus, slightly posterior and inferior to the MF (Fig. 6, bottom). This would suggest a more tangential orientation for the MEFII source, consistent with our observation that the MEFII produced relatively large pseudo-Z values in most subjects, even those showing a relatively weak MF. A precentral gyrus source of the MEFII also agrees with an increased excitability of the motor cortex observed at approximately the same latency in a transcranial magnetic stimulation (TMS) study of thumb movements [Chen et al., 1998]. It is interesting to speculate on the physiological mechanisms underlying the MEFII. Since this component peaks shortly after movement onset, it may reflect motor output related to ongoing motor control, such as onset of the antagonist burst (i.e., braking function), or it may reflect proprioceptive feedback from the periphery (possibly via area 2) known to activate neurons in MI [Lemon, 1979]. However, MEFII latency in the current study involving rather small (~1 cm) displacements of the finger is

similar to that reported in other studies utilizing much larger movements [Kristeva et al., 1991] and MEFII responses have been observed independently of whether finger flexion was followed by return of the finger to its original position [Holroyd et al., 1999]. This might suggest that the MEFII reflects activation of neuronal populations in MI as part of a centrally programmed motor pattern [Sanes and Jennings, 1984] and is independent of the timing of proprioceptive feedback. A alternative interpretation is that the anterior and posterior locations for the MF and MEFII sources may be related to the recent identification of cytoarchitectonically distinct anterior and posterior regions of the primary motor cortex in humans (areas 4a and 4p) that appear to contain functionally independent somatotopic representations of the digits [Geyer et al., 1996]. Interestingly, the latter study reported activation of area 4p to be strongly associated with tasks involving tactile discrimination, and both areas 4a and 4p were activated during a button-pressing task.

Ipsilateral Motor Fields

The neural sources contributing to premovement magnetic fields have been debated in the literature, particularly with respect to the role of the ipsilateral motor cortex. Cheyne and colleagues [Cheyne and Weinberg, 1989; Kristeva et al., 1991] were the first to propose involvement of the ipsilateral primary motor cortex in the generation of bilateral motor fields as a possible reflection of the inhibition of associated or mirror movements—a view supported by TMS studies showing transcallosal inhibitory connections between cortical motor areas [Ferbert et al., 1992; Kobayashi et al., 2003; Netz et al., 1995]. However, a recent MEG study using a multiple dipole modeling approach suggested that ipsilateral motor fields were generated by sources in more anteriorly located premotor areas of the ipsilateral hemisphere [Huang et al., 2004]. Neuroimaging studies using fMRI or PET have also provided somewhat conflicting results regarding the activation of the ipsilateral motor areas during voluntary movements. Kim et al. [1993] were the first to show activation of the both contralateral and ipsilateral primary motor cortex during a finger- tapping task. However, other studies have reported only weak or inconsistent activation of ipsilateral MI for simple movements [Alkadhi et al., 2002], or dependence on complexity of the motor task [Nirkko et al., 2001] or handedness [Kobayashi et al., 2003; Li et al., 1996]. Other studies have shown ipsilateral activation of outside of the primary motor cortex [Cramer et al., 1999], decreased BOLD responses during movement relative to rest, i.e., "deactivation" [Allison et al., 2000], or even a combination of both [Nirkko et al., 2001]. The observation of deactivation of MI during ipsilateral movements is of particular interest since it lends support to the hypothesis of transcallosal inhibitory input to the ipsilateral motor cortex during unilateral movements [Allison et al., 2000; Nirkko et al., 2001].

Neuroimaging studies using fMRI or PET are difficult to compare directly to our results, due to the use of blocked designs and continuous motor tasks that may temporally blur activation related to movement preparation and that resulting from the sensory consequences of the movements. Moreover, many fMRI studies may not clearly separate precentral and postcentral gyrus activation [Nirkko et al., 2001]. In the current study, robust activation of the ipsilateral precentral gyrus could be clearly observed in individual subjects, as shown in Figure 3B. In addition, locations of the precentral gyrus sources for ipsilateral movements in the group results were similar and even slightly posterior to those for contralateral movements (Table II). These findings are in disagreement with those by Huang et al. [2004], who suggested that the ipsilateral MF originates from anterior premotor areas (PMA). However, it is important to note that we observed separate activity in the ipsilateral PMA, separate from activation of the precentral gyrus, as shown in Figure 5, for both left and right index finger movements. This suggests that dipole models of premovement activity may be biased by unaccounted for PMA activity within the same hemisphere. This may also explain the reported spatial variability of ipsilateral MF sources. This would be particularly true for weaker activations in the ipsilateral hemisphere, in comparison to the much larger amplitude contralateral precentral source that would likely be more successfully modeled as a single dipole. However, as noted by Huang et al. [2004], the presence of additional PMA activity in the contralateral hemisphere may also result in bias of MF source localization to more anterior locations when modeled as a single dipole.

Activation of Nonprimary Motor Areas

One of the more significant results of the ER-SAM method was the identification of additional generators of premovement magnetic fields in nonprimary motor areas. Somewhat unexpectedly, the strongest of these was activation of a region of left inferior parietal lobe (IPL), near the inferior portion of the postcentral gyrus, which was independent of the side of movement. This source showed a very similar time course for both right and left index finger movements, and was earlier in onset and longer in duration than ipsilateral motor cortex sources. Interestingly, an activation of the left inferior parietal cortex with a similar time course was also reported in an EEG study using a minimum-norm source reconstruction [Ball et al., 1999]. Additionally, a recent fMRI study found increased activation of the left inferior parietal lobe for self-paced movements in comparison to externally triggered movements [Wiese et al., 2004]. However, both of these studies only examined right index finger movements, whereas we observed early left IPL activity for both left- and right-sided movements, consistent with specialization of the left hemisphere in motor control. This area is more anterior to those regions of the parietal lobe (e.g., supramarginal gyrus) associated with movement selection or visuomotor transformations [Rushworth et al., 1997] and it has been suggested that this might represent attentional aspects of motor preparation acting as a "motor intention" area [Andersen et al., 1997; Ball et al., 1999]. Alternatively,

since these simple motor tasks required pressing a button without visual feedback, this area may be related to the control of movements utilizing haptic, rather than visual guidance [Grezes and Decety, 2001]. This would be consistent with our observation of a ventral portion of the premotor area of the left hemisphere that has been implicated in a frontoparietal network controlling the manipulation of objects [Binkofski et al., 1999]. It is interesting to note that the left PMA and left inferior parietal areas showed similar time courses of activity in the current study. However, we observed bilateral activation of premotor areas for both left and right movement, with somewhat weaker activation of both left and right PMA for left index finger movements. Since all our subjects were right-handed, this might reflect differences in preparation or strategy for performing skilled movements with the nondominant hand, and is consistent with previous observations of the effects of handedness on movement-related neuromagnetic fields [Taniguchi et al., 1998].

The weakest and least consistent activation was found in the SMA located in the left superior mesial cortex, most likely corresponding to previously reported movement-related activation of the posterior SMA [Babiloni et al., 2001; Ball et al., 1999]. Attempts to measure SMA activity with neuromagnetic recordings have proven difficult and it has been suggested that this is due to the attenuation of simultaneously active areas of cortex on the mesial surface of the frontal lobes [Cheyne and Weinberg, 1989]. This hypothesis was supported by the observation of SMA sources in a patient with a unilateral lesion of the SMA [Lang et al., 1991]. More recent studies have measured activity of the SMA during the very early premovement period when these weaker sources are presumably less obscured by stronger activity in the neighboring sensorimotor cortex [Erdler et al., 2000]. Our current results partially support these findings by showing a relatively early onset of the SMA source for right index finger movements that decreased in activity just prior to movement onset, although this was not clearly replicated for left finger movements. It should be noted here that beamforming based spatial filters are relatively insensitive to highly correlated signals as well as extended sources [Vrba, 2002]. Thus, the SMA activity observed in the current study might reflect only the uncorrelated portion of an extended area of bilateral activation of the mesial cortex. These results need to be confirmed utilizing a greater numbers of trials, and more complex motor tasks that may increase activation of the SMA.

CONCLUSIONS

Localization of the underlying generators of movement-related fields presents a challenge to conventional source reconstruction methods used in MEG, due to the activation of multiple brain areas, and the contamination of the slowly changing premovement fields by interference from low-frequency noise of environmental and biological origin. We used a new analysis approach—event-related synthetic aperture magnetometry (ER-SAM)—to create 3D images of brain activity during voluntary movements with millisecond resolution and without the need to specify the number of neural sources. This method was found to be sufficiently unaffected by slow frequency noise artifacts (e.g., eye movements) to alleviate the need for extensive editing of individual subject data, and thus provides a robust localization method for slow magnetic field changes accompanying voluntary movement or other behavioral tasks. This has the potential of providing a practical method for neuromagnetic source localization in populations such as patients or young children where performance (e.g., ability to fixate) is often inadequate for the purpose of conventional source localization methods.

The ability of the current method to resolve multiple sources within the sensorimotor cortex may result from the use of the unaveraged MEG data to compute the beamformer weights, since it is known that increasing SNR will increase spatial resolution [Barnes and Hillebrand, 2003; Cheyne et al., 2004]. However, the derivation of the beamformer weights from the unaveraged data raises the question of the contribution of nontime-locked activity, such as induced or spontaneous oscillations, to both the selection of source orientation and the resulting spatial selectivity of the weights to other sources. This is of particular concern for the current study since robust 10 and 20 Hz oscillations are often observed in sensorimotor cortex during movement tasks [Cheyne and Gaetz, 2003; Salenius et al., 1997]. However, we observed slightly noisier but highly similar patterns of source activity in individual subjects when applying a more restrictive (8 Hz) low-pass filter, suggesting that higher frequency oscillations in the mu and beta frequency bands that may have been present in the single trial data did not play a role in focusing of the beamformer weights in the regions of source activity, and that the source activity localized in the ER-SAM images represents relatively low-frequency, transient brain events. In comparison, Hashimoto et al. [2001] described the time course of multiple postcentral gyrus sources of the early median nerve response using a vector beamformer derived from averaged MEG data. In the current study, we found that the use of the covariance matrix derived from the averaged measurements produced much noisier source images with spurious source peaks. However, the approach used by Hashimoto et al. differed in that they applied the resulting beamformer weights to only the estimated signal subspace of the measurement covariance matrix [Sekihara et al., 2001], possibly resulting in higher signal to noise of the resulting images, although this approach requires a priori specification of the dimension of this subspace (number of sources). In addition, as SNR increases (more averaging) or sample number decreases (shorter epochs) regularization may be required for the computation of the covariance matrix inverse which will decrease spatial resolution of the filter. The advantage of our current approach is that no user input is required other than selecting the region of interest and desired spatial resolution. Nevertheless, further studies are needed to determine the relative

merits of deriving beamforming weights from either spontaneous brain activity or averaged measurements.

Volumetric source imaging using ER-SAM lends itself easily to the use of existing spatial normalization and group averaging techniques [Singh et al., 2003], thereby increasing the ability to detect weaker sources of activity and group effects. Thus, we were able to demonstrate activity in nonprimary motor areas, including the premotor and parietal cortex, not previously reported in MEG studies of voluntary movements. One area for future work is the development of statistical thresholding techniques that are not overly conservative [Chau et al., 2004] due to the large variability in source amplitude in the ER-SAM images. We found that computing images based on the plus-minus averaged data provided a useful estimate of the amount of nonstimulus locked activity projected by the spatial filters [see also Robinson, 2004]. Finally, the ability to construct group averaged time courses (virtual sensors) for areas of peak activation allowed us to delineate the temporal patterns of activity of adjacent but independently active brain regions throughout the movement period.

ACKNOWLEDGMENTS

The authors thank Dr. Krish Singh for assistance with SAM spatial normalization and statistical methods, and for distribution of the mri3dX program, and Drs. Jiri Vrba and Steve Robinson for their helpful advice on beamforming methods.

REFERENCES

Alkadhi H, Crelier GR, Boendermaker SH, Hepp-Reymond MC, Kollias SS (2002): Somatotopy in the ipsilateral primary motor cortex. Neuroreport 13:2065–2070.

Allison JD, Meador KJ, Loring DW, Figueroa RE, Wright JC (2000): Functional MRI cerebral activation and deactivation during finger movement. Neurology 54:135–142.

Andersen RA, Snyder LH, Bradley DC, Xing J (1997): Multimodal representation of space in the posterior parietal cortex and its use in planning movements. Annu Rev Neurosci 20:303–330.

Babiloni F, Carducci F, Cincotti F, Del Gratta C, Pizzella V, Romani GL, Rossini PM, Tecchio F, Babiloni C (2001): Linear inverse source estimate of combined EEG and MEG data related to voluntary movements. Hum Brain Mapp 14:197–209.

Bakhtazad L, Gaetz W, Cheyne D (2004): High resolution neuromagnetic imaging using minimum-variance beamforming reveals multiple generators of movement-evoked fields. In: Halgren E, Ahlfors S, Hamalainen M, Cohen D, editors. Proc 14th Int Conf Biomagnetism. Boston: Biomag 2004. p 723.

Ball T, Schreiber A, Feige B, Wagner M, Lucking CH, Kristeva-Feige R (1999): The role of higher-order motor areas in voluntary movement as revealed by high-resolution EEG and fMRI. Neuroimage 10:682–694.

Bardouille T, Herdman AT, Chau W, Pantev C (2004): A spatiotemporal approach to cortical mapping using synthetic aperture magnetometry. Brain Cogn 54:175–176.

Barnes GR, Hillebrand A (2003): Statistical flattening of MEG beamformer images. Hum Brain Mapp 18:1–12.

Binkofski F, Buccino G, Posse S, Seitz RJ, Rizzolatti G, Freund H (1999): A fronto-parietal circuit for object manipulation in man: evidence from an fMRI-study. Eur J Neurosci 11:3276–3286.

Bocker KB, Brunia CH, Cluitmans PJ (1994): A spatio-temporal dipole model of the readiness potential in humans. I. Finger movement. Electroencephalogr Clin Neurophysiol 91:275–285.

Chau W, McIntosh AR, Robinson SE, Schulz M, Pantev C (2004): Improving permutation test power for group analysis of spatially filtered MEG data. Neuroimage 23:983–996.

Chen R, Yaseen Z, Cohen LG, Hallett M (1998): Time course of corticospinal excitability in reaction time and self-paced movements. Ann Neurol 44:317–325.

Cheyne D, Gaetz W (2003): Neuromagnetic localization of oscillatory brain activity associated with voluntary finger and toe movements. Neuroimage 19(Suppl):1061.

Cheyne D, Weinberg H (1989): Neuromagnetic fields accompanying unilateral finger movements: pre-movement and movement-evoked fields. Exp Brain Res 78:604–612.

Cheyne D, Weinberg H, Gaetz W, Jantzen KJ (1995): Motor cortex activity and predicting side of movement: neural network and dipole analysis of pre-movement magnetic fields. Neurosci Lett 188:81–84.

Cheyne D, Endo H, Takeda T, Weinberg H (1997): Sensory feedback contributes to early movement-evoked fields during voluntary finger movements in humans. Brain Res 771:196–202.

Cheyne D, Bakhtazad L, Gaetz W (2004): Effects of correlated brain activity on performance of minimum-variance beamformer and equivalent current dipole localization methods. In: Halgren E, Ahlfors S, Hamalainen M, Cohen D, editors. Proc 14th Int Conf Biomagnetism. Boston: Biomag 2004. p 488.

Collins DL, Neelin P, Peters TM, Evans AC (1994): Automatic 3D intersubject registration of MR volumetric data in standardized Talairach space. J Comput Assist Tomogr 18:192–205.

Cramer SC, Finklestein SP, Schaechter JD, Bush G, Rosen BR (1999): Activation of distinct motor cortex regions during ipsilateral and contralateral finger movements. J Neurophysiol 81:383–387.

Erdler M, Beisteiner R, Mayer D, Kaindl T, Edward V, Windischberger C, Lindinger G, Deecke L (2000): Supplementary motor area activation preceding voluntary movement is detectable with a whole-scalp magnetoencephalography system. Neuroimage 11:697–707.

Fawcett IP, Barnes GR, Hillebrand A, Singh KD (2004): The temporal frequency tuning of human visual cortex investigated using synthetic aperture magnetometry. Neuroimage 21:1542–1553.

Ferbert A, Priori A, Rothwell JC, Day BL, Colebatch JG, Marsden CD (1992): Interhemispheric inhibition of the human motor cortex. J Physiol 453:525–546.

Fink GR, Frackowiak RS, Pietrzyk U, Passingham RE (1997): Multiple nonprimary motor areas in the human cortex. J Neurophysiol 77:2164–2174.

Gaetz WC, Cheyne DO (2003): Localization of human somatosensory cortex using spatially filtered magnetoencephalography. Neurosci Lett 340:161–164.

Ganslandt O, Fahlbusch R, Nimsky C, Kober H, Moller M, Steinmeier R, Romstock J, Vieth J (1999): Functional neuronavigation with magnetoencephalography: outcome in 50 patients with lesions around the motor cortex. J Neurosurg 91:73–79.

Geyer S, Ledberg A, Schleicher A, Kinomura S, Schormann T, Burgel U, Klingberg T, Larsson J, Zilles K, Roland PE (1996): Two different areas within the primary motor cortex of man. Nature 382:805–807.

Grezes J, Decety J (2001): Functional anatomy of execution, mental simulation, observation, and verb generation of actions: a meta-analysis. Hum Brain Mapp 12:1–19.

Gross J, Kujala J, Hamalainen M, Timmermann L, Schnitzler A, Salmelin R (2001): Dynamic imaging of coherent sources: Studying neural interactions in the human brain. Proc Natl Acad Sci U S A 98:694–699.

Gross J, Pollok B, Dirks M, Timmermann L, Butz M, Schnitzler A (2005): Task-dependent oscillations during unimanual and bimanual movements in the human primary motor cortex and SMA studied with magnetoencephalography. Neuroimage 26: 91–98.

Hanakawa T, Parikh S, Bruno MK, Hallett M (2004): Finger and face representations in the ipsilateral precentral motor areas in humans. J Neurophysiol 93:2950–2958.

Hashimoto I, Kimura T, Iguchi Y, Takino R, Sekihara K (2001): Dynamic activation of distinct cytoarchitectonic areas of the human SI cortex after median nerve stimulation. Neuroreport 12:1891–1897.

Hashimoto I, Kimura T, Tanosaki M, Iguchi Y, Sekihara K (2003): Muscle afferent inputs from the hand activate human cerebellum sequentially through parallel and climbing fiber systems. Clin Neurophysiol 114:2107–2117.

Herdman AT, Wollbrink A, Chau W, Ishii R, Pantev C (2004): Localization of transient and steady-state auditory evoked responses using synthetic aperture magnetometry. Brain Cogn 54:149–151.

Hillebrand A, Barnes GR (2003): The use of anatomical constraints with MEG beamformers. Neuroimage 20:2302–2313.

Hirata M, Kato A, Taniguchi M, Ninomiya H, Cheyne D, Robinson SE, Maruno M, Kumura E, Ishii R, Hirabuki N, Nakamura H, Yoshimine T (2002): Frequency-dependent spatial distribution of human somatosensory evoked neuromagnetic fields. Neurosci Lett 318:73–76.

Holroyd T, Endo H, Kelso JAS, Takeda T (1999): Dynamics of the MEG recorded during rhythmic index-finger extension and flexion. In: Yoshimoto T, Kotani M, Kuriki S, Nakasato N, Karibe H, editors. Recent advances in biomagnetism. Proc 11th Int Conf Biomagnetism. Tohoku University Press. p 446–449.

Huang MX, Mosher JC, Leahy RM (1999): A sensor-weighted overlapping-sphere head model and exhaustive head model comparison for MEG. Phys Med Biol 44:423–440.

Huang MX, Harrington DL, Paulson KM, Weisend MP, Lee RR (2004): Temporal dynamics of ipsilateral and contralateral motor activity during voluntary finger movement. Hum Brain Mapp 23:26–39.

Joliot M, Papathanassiou D, Mellet E, Quinton O, Mazoyer N, Courtheoux P, Mazoyer B (1999): FMRI and PET of self-paced finger movement: comparison of intersubject stereotaxic averaged data. Neuroimage 10:430–447.

Kakigi R, Hoshiyama M, Shimojo M, Naka D, Yamasaki H, Watanabe S, Xiang J, Maeda K, Lam K, Itomi K et al. (2000): The somatosensory evoked magnetic fields. Prog Neurobiol 61:495–523.

Kim SG, Ashe J, Georgopoulos AP, Merkle H, Ellermann JM, Menon RS, Ogawa S, Ugurbil K (1993): Functional imaging of human motor cortex at high magnetic field. J Neurophysiol 69:297–302.

Kobayashi M, Hutchinson S, Schlaug G, Pascual-Leone A (2003): Ipsilateral motor cortex activation on functional magnetic resonance imaging during unilateral hand movements is related to interhemispheric interactions. Neuroimage 20:2259–22570.

Kristeva R, Cheyne D, Deecke L (1991): Neuromagnetic fields accompanying unilateral and bilateral voluntary movements: topography and analysis of cortical sources. Electroencephalogr Clin Neurophysiol 81:284–298.

Kristeva-Feige R, Rossi S, Pizzella V, Tecchio F, Romani GL, Erne S, Edrich J, Orlacchio A, Rossini PM (1995): Neuromagnetic fields of the brain evoked by voluntary movement and electrical stimulation of the index finger. Brain Res 682:22–28.

Kristeva-Feige R, Rossi S, Pizzella V, Sabato A, Tecchio F, Feige B, Romani GL, Edrich J, Rossini PM (1996): Changes in movement-related brain activity during transient deafferentation: a neuromagnetic study. Brain Res 714:201–208.

Lancaster JL, Woldorff MG, Parsons LM, Liotti M, Freitas CS, Rainey L, Kochunov PV, Nickerson D, Mikiten SA, Fox PT (2000): Automated Talairach atlas labels for functional brain mapping. Hum Brain Mapp 10:120–131.

Lang W, Cheyne D, Kristeva R, Beisteiner R, Lindinger G, Deecke L (1991): Three-dimensional localization of SMA activity preceding voluntary movement. A study of electric and magnetic fields in a patient with infarction of the right supplementary motor area. Exp Brain Res 87:688–695.

Lemon RN (1979): Short-latency peripheral inputs to the motor cortex in conscious monkeys. Brain Res 161:150–155.

Li A, Yetkin FZ, Cox R, Haughton VM (1996): Ipsilateral hemisphere activation during motor and sensory tasks. AJNR Am J Neuroradiol 17:651–655.

Nagamine T, Kajola M, Salmelin R, Shibasaki H, Hari R (1996): Movement-related slow cortical magnetic fields and changes of spontaneous MEG- and EEG-brain rhythms. Electroencephalogr Clin Neurophysiol 99:274–286.

Netz J, Ziemann U, Homberg V (1995): Hemispheric asymmetry of transcallosal inhibition in man. Exp Brain Res 104:527–533.

Nichols TE, Holmes AP (2002): Nonparametric permutation tests for functional neuroimaging: a primer with examples. Hum Brain Mapp 15:1–25.

Nirkko AC, Ozdoba C, Redmond SM, Burki M, Schroth G, Hess CW, Wiesendanger M (2001): Different ipsilateral representations for distal and proximal movements in the sensorimotor cortex: activation and deactivation patterns. Neuroimage 13:825–835.

Oishi M, Kameyama S, Fukuda M, Tsuchiya K, Kondo T (2004): Cortical activation in area 3b related to finger movement: an MEG study. Neuroreport 15:57–62.

Pedersen JR, Johannsen P, Bak CK, Kofoed B, Saermark K, Gjedde A (1998): Origin of human motor readiness field linked to left middle frontal gyrus by MEG and PET. Neuroimage 8:214–220.

Pollok B, Gross J, Muller K, Aschersleben G, Schnitzler A (2005): The cerebral oscillatory network associated with auditorily paced finger movements. Neuroimage 24:646–655.

Robinson SE (2004): Localization of event-related activity by SAM(erf). Proc 14th Int Conf Biomagnetism. Boston, MA. p 583–584.

Robinson SE, Vrba J (1999): Functional neuroimaging by synthetic aperture magnetometry. In: Yoshimine T, Kotani M, Kuriki S, Karibe H, Nakasato N, editors. Recent Advances in Biomagnetism: Proceedings From the 11th International Conference on Biomagnetism. Sendai: Tokoku University Press. p 302–305.

Rushworth MF, Nixon PD, Passingham RE (1997): Parietal cortex and movement. I. Movement selection and reaching. Exp Brain Res 117:292–310.

Salenius S, Schnitzler A, Salmelin R, Jousmaki V, Hari R (1997): Modulation of human cortical rolandic rhythms during natural sensorimotor tasks. Neuroimage 5:221–228.

Sanes JN, Jennings VA (1984): Centrally programmed patterns of muscle activity in voluntary motor behavior of humans. Exp Brain Res 54:23–32.

Sarvas J (1987): Basic mathematical and electromagnetic concepts of the biomagnetic inverse problem. Phys Med Biol 32:11–22.

Schulz M, Chau W, Graham SJ, McIntosh AR, Ross B, Ishii R, Pantev C (2004): An integrative MEG-fMRI study of the primary somatosensory cortex using cross-modal correspondence analysis. Neuroimage 22:120–133.

Sekihara K, Nagarajan SS, Poeppel D, Marantz A, Miyashita Y (2001): Reconstructing spatio-temporal activities of neural sources using an MEG vector beamformer technique. IEEE Trans Biomed Eng 48:760–771.

Sekihara K, Nagarajan SS, Poeppel D, Marantz A (2004): Asymptotic SNR of scalar and vector minimum-variance beamformers for neuromagnetic source reconstruction. IEEE Trans Biomed Eng 51:1726–1734.

Singh KD, Barnes GR, Hillebrand A (2003): Group imaging of task-related changes in cortical synchronisation using nonparametric permutation testing. Neuroimage 19:1589–1601.

Taniguchi M, Yoshimine T, Cheyne D, Kato A, Kihara T, Ninomiya H, Hirata M, Hirabuki N, Nakamura H, Hayakawa T (1998): Neuromagnetic fields preceding unilateral movements in dextrals and sinistrals. Neuroreport 9:1497–1502.

Taniguchi M, Kato A, Fujita N, Hirata M, Tanaka H, Kihara T, Ninomiya H, Hirabuki N, Nakamura H, Robinson SE et al. (2000): Movement-related desynchronization of the cerebral cortex studied with spatially filtered magnetoencephalography. Neuroimage 12:298–306.

Toma K, Matsuoka T, Immisch I, Mima T, Waldvogel D, Koshy B, Hanakawa T, Shill H, Hallett M (2002): Generators of movement-related cortical potentials: fMRI-constrained EEG dipole source analysis. Neuroimage 17:161–173.

Toro C, Matsumoto J, Deuschl G, Roth BJ, Hallett M (1993): Source analysis of scalp-recorded movement-related electrical potentials. Electroencephalogr Clin Neurophysiol 86:167–175.

Van Veen BD, van Drongelen W, Yuchtman M, Suzuki A (1997): Localization of brain electrical activity via linearly constrained minimum variance spatial filtering. IEEE Trans Biomed Eng 44:867–880.

Volkmann J, Schnitzler A, Witte OW, Freund H (1998): Handedness and asymmetry of hand representation in human motor cortex. J Neurophysiol 79:2149–2154.

Vrba J (2002): Magnetoencephalography: the art of finding a needle in a haystack. Physica C 368:1–9.

Vrba J, Robinson SE (2001): Signal processing in magnetoencephalography. Methods (Duluth) 25:249–271.

Wiese H, Stude P, Nebel K, de Greiff A, Forsting M, Diener HC, Keidel M (2004): Movement preparation in self-initiated versus externally triggered movements: an event-related fMRI-study. Neurosci Lett 371:220–225.

Woldag H, Waldmann G, Schubert M, Oertel U, Maess B, Friederici A, Hummelsheim H (2003): Cortical neuromagnetic fields evoked by voluntary and passive hand movements in healthy adults. J Clin Neurophysiol 20:94–101.

Yousry TA, Schmid UD, Alkadhi H, Schmidt D, Peraud A, Buettner A, Winkler P (1997): Localization of the motor hand area to a knob on the precentral gyrus. A new landmark. Brain 120:141–157.